MICCS: A Fully Programmable Multipurpose Integrated Cell Culture System

Timothy Kassis[1, 3], Paola M. Perez[1], Chloe J.W. Yang[1], Luis R. Soenksen[2], David L. Trumper[2,3,*] & Linda G. Griffith[1,*]

[1] Department of Biological Engineering
[2] Department of Mechanical Engineering
[3] Research Laboratory of Electronics

Massachusetts Institute of Technology, Cambridge, MA

* Corresponding authors.

Abstract

With the rise of research utilizing microphysiological systems (MPSs), the need for tools that enable the physiological mimicking of the relevant cellular environment is vital. The inability to reproduce crucial features of the microenvironment, such as surrounding fluid flow and dynamic changes in biochemical stimuli, severely limits the type of experiments that can be carried out. Unfortunately, current equipment to achieve this is expensive, large, difficult to control and has limited potential for scalability. Here, we present the Multipurpose Integrated Cell Culture System (MICCS) – an open-source, low-cost, modular, scalable, fully-programmable and easy to assemble pumping platform that can be incorporated into cell culture systems to better recapitulate physiological environments. By using two commercially available piezoelectric pumps, MICCS is capable of producing arbitrarily dynamic flow profiles with reliable flow rates ranging from 1 to 3,000 µL/min as specified by the easily programmable user input. We validated the accuracy of the flow rates, the use of dynamic profiles, and the practicality of the platform by using it to successfully create repeatable dynamic concentration profiles.

Introduction

With the rise of organ-on-chips (OOC) and microphysiological systems (MPS)[1–11], the ability to mimic the highly dynamic cellular microenvironment has become crucial in allowing these systems to recapitulate *in vivo* physiological responses[12]. Two critical factors involved in mimicking the cellular microenvironment are dynamic flow rates and variable concentration profiles of hormones, proteins, sugars and other biochemical stimuli[13]. For example, mechanical stimuli, such as flow-induced wall shear stress[14,15], and biochemical stimuli, such as varying hormone levels, have been shown to dramatically improve the functionality of these *in vitro* model systems and their physiological relevancy. While there are numerous techniques to impose flow in microfluidic setups[16], existing methods face certain limitations. Continuously imposing adequate flow for long period of time requires large and complex setups that involve external syringe pumps, peristaltic pumps or the use of one of the numerous commercialized microfluidic pumps that utilize pressure-driven flow. While each of these configurations offers certain advantages, they are typically expensive, tedious to assemble and setup, allow for limited programmability, and do not generally lend themselves as scalable solutions.

There have been numerous attempts made recently by both academics and commercial entities to address some of these limitations[16–27]. Here we present a microfluidic pumping platform designed to offer greater experimental flexibility, ease of assembly, high scalability and customized flow-rate programmability compared to other currently available commercial and academic systems. Our modular Multipurpose Integrated Cell Culture System (MICCS) incorporates two commercially available piezoelectric pumps[28] capable of reliable flow rates ranging from 1 to 3,000 µL/min. The pumps are controlled via a Wi-Fi enabled Raspberry Pi Zero microcontroller and can be accessed remotely while in the incubator using a remote server. The entire system has a minimal footprint, and the 3D printed casing is designed to make the devices stackable. Because of the low power requirements, the system can be battery operated, thus allowing for mobility and uninterrupted flow during day-to-day use as well as eliminating the need for external connections to the cell culture incubator. We demonstrated the system's utility by integrating it with a custom-designed microfluidic mixer and by programmatically controlling the flow-rates on both pumps to create dynamic concentration profiles that can potentially be used to impose time-varying concentrations of hormones, drugs or other biochemical stimuli in the designated OOC or MPS on time scales ranging from seconds to weeks.

Materials and Methods

Pump Control and PCB Design

MICCS is composed of two piezoelectric pumps, two pump driving circuits, two connectors, a printed circuit board (PCB) and a microcontroller (Fig. 1). The Bartels Microtechnik mp6 piezoelectric pumps (Servoflo, Lexington, MA) were chosen due to their small size, reliability, high dynamic range, low power consumption (< 200 mW), long operating life-time (~5,000 hrs) and chemical compatibility. Each pump has a single barbed inlet and outlet (OD = 1.9 mm) making it easy to interface to using readily available standard commercial tubing. Two commercially available mp6-OEM driving circuits (Servoflo) were used in conjunction with a Raspberry Pi Zero W (Adafruit, NY) running Raspbian Jessie Linux distribution to control both pumps. The driving circuits generate a 270 V_{pp} voltage from the 3.3 V supply voltage of the microcontroller and can be used to control both the amplitude and frequency of actuation. We found that controlling just the frequency was adequate. The frequency was set using a software pulse-width modulated (PWM) signal with a duty cycle of 95% generated by two output pins of the Pi and supplied to each of the CLOCK pins of the mp6-OEM. A custom-built PCB along with two 1.25 mm pitch Molex connectors (Molex, IL) were used to connect all the various components (See supplemental material for PCB layout).

Operating Code

Python 3.5 along with the Raspberry Pi GPIO library were used to control a software PWM signal generated through the Raspberry Pi Zero W. The frequency of the PWM was modulated to control the flow rate. Two different output pins were used to generate a PWM signal for each pump. A calibration curve (frequency vs. flow-rate) was created to determine the PWM signal corresponding to each flow rate. A small Python library was developed with two main functions: *Constant_Flow(Q1,Q2,T)* generates a constant flow rate (Q1 and Q2 for pumps 1 and 2 respectively) for a specified duration (T in sec), and *Dynamic_Flow(csv_path)* takes in a file path for a comma separated ".csv" file. The csv file contains three columns with the sampling interval in seconds in the first column and the flow rates, in µL/min for each pump, in the next two columns (example ".csv" file in supplemental). The ".csv" file can be generated by the user to perform any custom pump functionality by dynamically controlling both pumps. All Python code used in this paper is available at https://github.com/TKassis/MICCS and can be downloaded directly to the Raspberry Pi.

Flow Rate Calibration and Validation

The pump flow-rate is set by specifying a PWM signal with a certain frequency. A calibration curve was created by weighing the total pumped volume, given a certain frequency input, of ultra-filtered water for

selected time intervals. Each measurement was repeated three times. A calibration curve was created for each pump separately. The flow-rates were then validated under the same conditions in which the subsequent experiments would take place. For the flow validation experiments, the mass of water was measured for 10-minute flow intervals and measurements were repeated four times for each prescribed flow rate.

3D Printed Casing

The casing and the sliding mechanisms were designed using Autodesk Fusion 360, exported as an STL file and printed with standard resin (gray or clear) on a Form 2 3D printer (Formlabs, Somerville, MA) at a set vertical resolution of 50 µm. The print was then soaked in Isopropyl Alcohol (IPA) for 20 minutes, and then dried with an air gun. After removing the support structures, the casing was post-cured under UV light for 1 hour using a Salon Edge 36W Professional UV dryer (Amazon). The CAD file, in both STEP and STL formats, is included in the supplemental files.

Mixer Fabrication and Validation

The mixer was made from poly(dimethylsiloxane) (PDMS) bound to a glass slide (See supplemental files for the CAD file in both STEP and STL formats). The mold was designed using Autodesk Fusion 360, exported as an STL file and printed with standard clear resin on a Form 2 3D printer at a set vertical resolution of 25 µm. The print was then soaked in IPA for 20 minutes, washed thoroughly with fresh IPA, and then dried with an air gun. After removing the support structures, the mold was post-cured under UV light for 1 hour using a Salon Edge 36W Professional UV dryer. To construct a device, PDMS was thoroughly mixed in a 10:1 ratio of base to curing agent (Sylgard 184, Dow Corning), poured into the mold, degassed for 20 minutes using a vacuum chamber, and then cured at 60 °C for a minimum of 8 hours. The first time a new mold was used, PDMS did not fully cure due to resin leaching out of the 3D print and was therefore discarded. After the initial batch was discarded, subsequent devices were successfully manufactured. Devices were then punched with a 1 mm biopsy punch to create inlet and outlet holes for tubing, cleaned with scotch tape, air plasma treated for 30-60 seconds, immediately bonded to 1 mm thick glass slides, then left in an oven at 60 °C for minimum of 2 hours to strengthen the PDMS-glass bonds. The mixers were sterilized by soaking them in 70% ethanol for 5 minutes, then rinsing thoroughly with sterile deionized water. Before use, mixers were filled with 1% bovine serum albumin (BSA) solution for 1 hour to decrease non-specific binding. To validate the mixing efficiency of the static mixer we conducted 2D multi-physics simulations using COMSOL 5.2a . The study was composed of two COMSOL simulation steps. For the first step, we solved a discretized (P2 + P1) laminar flow simulation where the inlet velocity (0.055 m/s) for each of the inlets was specified to equal the flow rate we utilized for the concentration validation

experiments (400 µL/min to each inlet). The second step utilized the laminar flow solution and a discretized quadratic transport of dilute species study to solve for mixing throughout the device given a diffusion coefficient of 4.25×10^{-10} m^2/s for fluorescein[29]. The concentration of fluorescein was set to 1 mol/m^3 for the high-concentration inlet while the other inlet had pure water. We utilized a parametric sweep for the dynamic concentration simulation given the inlet velocities from our prescribed ".csv" file.

Concentration Profile Validation

Two 250 mL bottles were filled with deionized water and deionized water with stock concentration of fluorescein respectively. The setup, using MICCS connected to the mixer, was placed in a temperature-controlled incubation chamber in a Zeiss LSM 880 confocal microscope. Images were acquired every 5 seconds with a resolution of 512x512 using ZEN Black confocal software (Zeiss) and at a 16-bit depth resolution. The images were saved as .czi files. Each file was loaded into the open-source image processing software, Fiji, and fluorescence intensity was measured using Fiji's built-in region of interest (ROI) intensity measurement functionality. The ROI was drawn as a small rectangle in the center of the outlet channel of the mixer. The intensity measurement that Fiji calculated was the mean intensity of all the pixels within the ROI. Using a calibration curve (mean fluorescence intensity vs. fluorescein concentration) that was created using the same setup for known fluorescein concentrations the final concentration values were determined from the fluorescence intensity.

Results and Discussion

A Feature-Rich Modular Pumping System for Lab-on-a-Chip Applications

MICCS is a valuable system for a wide variety of both biological and non-biological fluidic applications. We designed MICCS to address many of the limitations that we ourselves encounter every day when working with external pumping systems for microfluidic devices. While commercially available flow systems can offer numerous benefits, systems such as syringe and peristaltic pumps have always been cumbersome to use, have a large footprint, thus making them non-scalable, are difficult if not impossible to program, and are costly for biological experiments that require a high number of replicates and sample conditions. To address these limitations we set out to design a pumping platform specifically geared towards flexibility, programmability, and scalability. The result was a modular pumping system where each module is composed of two piezoelectric pumps, two driving circuits, a custom designed PCB and a 3D printed casing (Fig. 1A). Having two pumps on each platform greatly expands the utility of the system as it allows for applications involving multiple flow rates such microphysiological systems with apical and basal flow, and two-solute mixing applications. Each module is controlled using a single Raspberry Pi Zero W

computer that offers a full-fledged Linux operating system and Wi-Fi capabilities. This permitted us to remotely access the MICCS module using a VNC server free of charge (see the official Raspberry Pi documentation for using RealVNC.com) while the system is in the incubator, thus allowing both real-time monitoring and full programming capabilities using a number of languages such as Python, Scratch, JAVA, C and C++. MICCS allows the user to create Python scripts that control flow rates for each pump individually which greatly reducing user intervention in biological experiments by potentially automating many fluid addition and exchange tasks. The pump control scripts that we developed for the module were all in Python and are available with an open source license[30,31]. Each module has a small footprint measuring 122x42 mm (Fig. 1B) that makes it easy to handle and to place in a cell culture incubator with no external wiring or tubing if using an external USB power-pack. While not shown here, we demonstrated that the entire electronic assembly is robust to the high humidity found in a typical cell incubator by running the platform continuously for a week without any perceived side effects to the hardware or reduction in performance (n=2). Additionally, the pump material that is in fluid contact is biocompatible where the inner surface of the pump is made from polyphenylene sulphone (PSSU) and is both sterilizable using 70% ethanol and autoclavable. We designed the casing with a sliding mechanism that allows the user to stack multiple modules on top of each other depending on how many total pumps are required (Fig. 1C). The end result is a cheap (<$200), fully programmable, remotely-accessible, battery-operated, scalable and easy-to-operate pumping platform that can be utilized for a variety of fluidic applications.

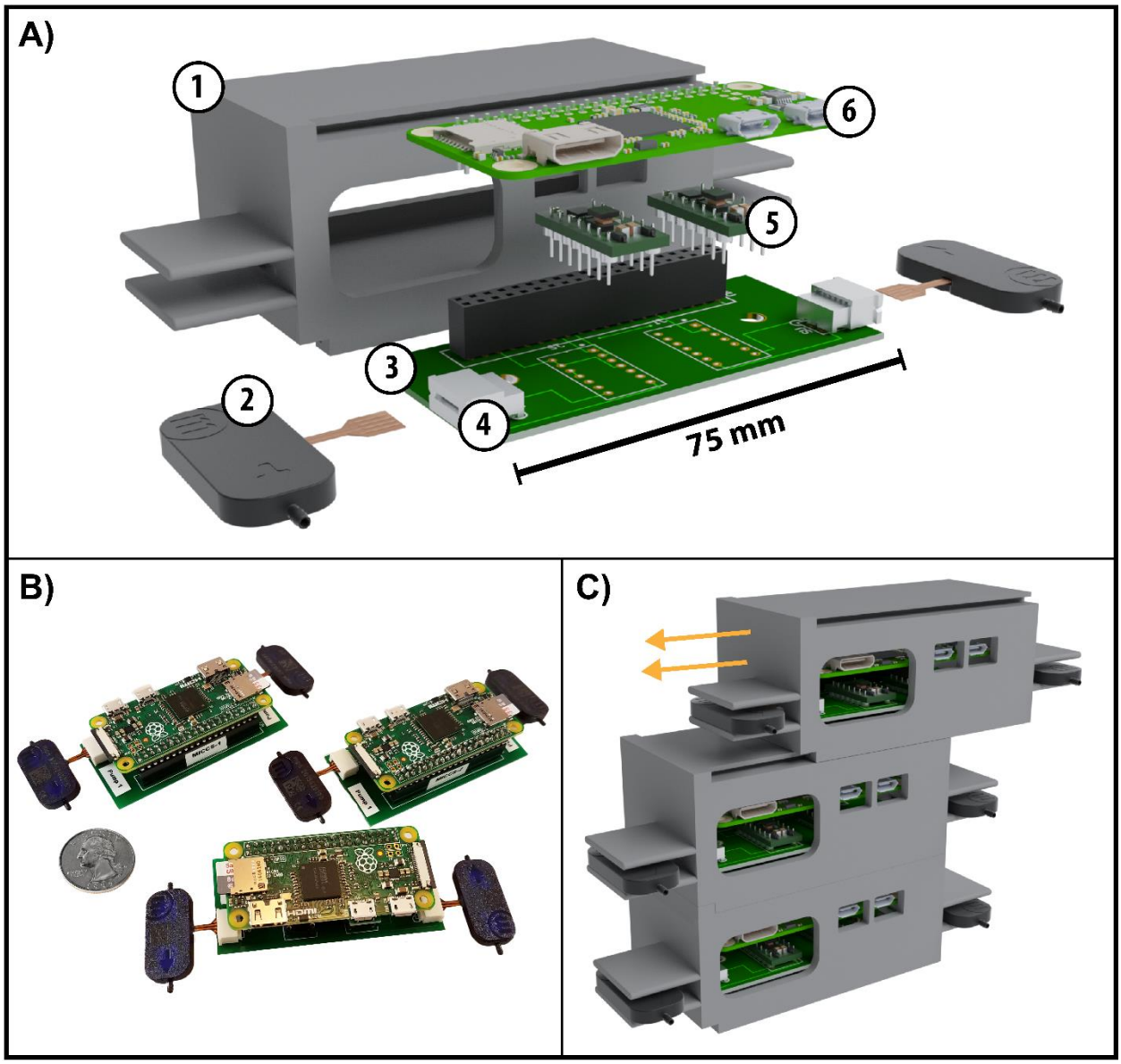

***Figure 1: Overview of the Multipurpose Integrated Cell Culture System (MICCS)**. **A)** (1) An exploded rendering of the complete module showing a 3D printed case, (2) the commercially available mp6 piezoelectric pumps, (3) the custom designed PCB, (4) pump connectors, (5) commercially available driving circuits and (6) the Wi-Fi enabled Raspberry Pi Zero Linux computer. **B)** A US quarter next to three modules to show the small footprint. Each module can be given a host name and accessed remotely via a remote server free of charge (using RealVNC.com). **C)** The casing allows the modules to be easily stacked when more than two pumps are required. Given the cost, ease of assembly and size of the footprint of MICCS, it is possible to fit several dozen modules inside a typical cell culture incubator.*

Calibration Offers Reliable and Reproducible Flow Rates with a High Dynamic Range

The two pumps on each MICCS module were calibrated separately. While the two calibration curves showed the same linear trend, there is a small gain difference between them which requires each pump to have its own calibration curve. While it is not clear why this difference exists, it is most likely due to

manufacturing variability of the pump geometry. The calibration data shows a linear response up to 100 Hz, at which point there is an abrupt change in slope. To account for the change in slopes, we divided the curve into two sections. We fit a straight line through each set of data points where the first line was from 0-100 Hz and the second line was from 100-300 Hz (Fig. 2A,B). The calibration values were subsequently used in the pump control code. We validated the resulting code by measuring the flow rate using mass of water collected over a 10-min period for one of the pumps (Fig. 2C), and we found the flow rate to be highly accurate even at low flow rates (Fig. 2D). The validated flow rates illustrate the high dynamic range possible with MICCS, ranging from 1 to 3000 µL/min.

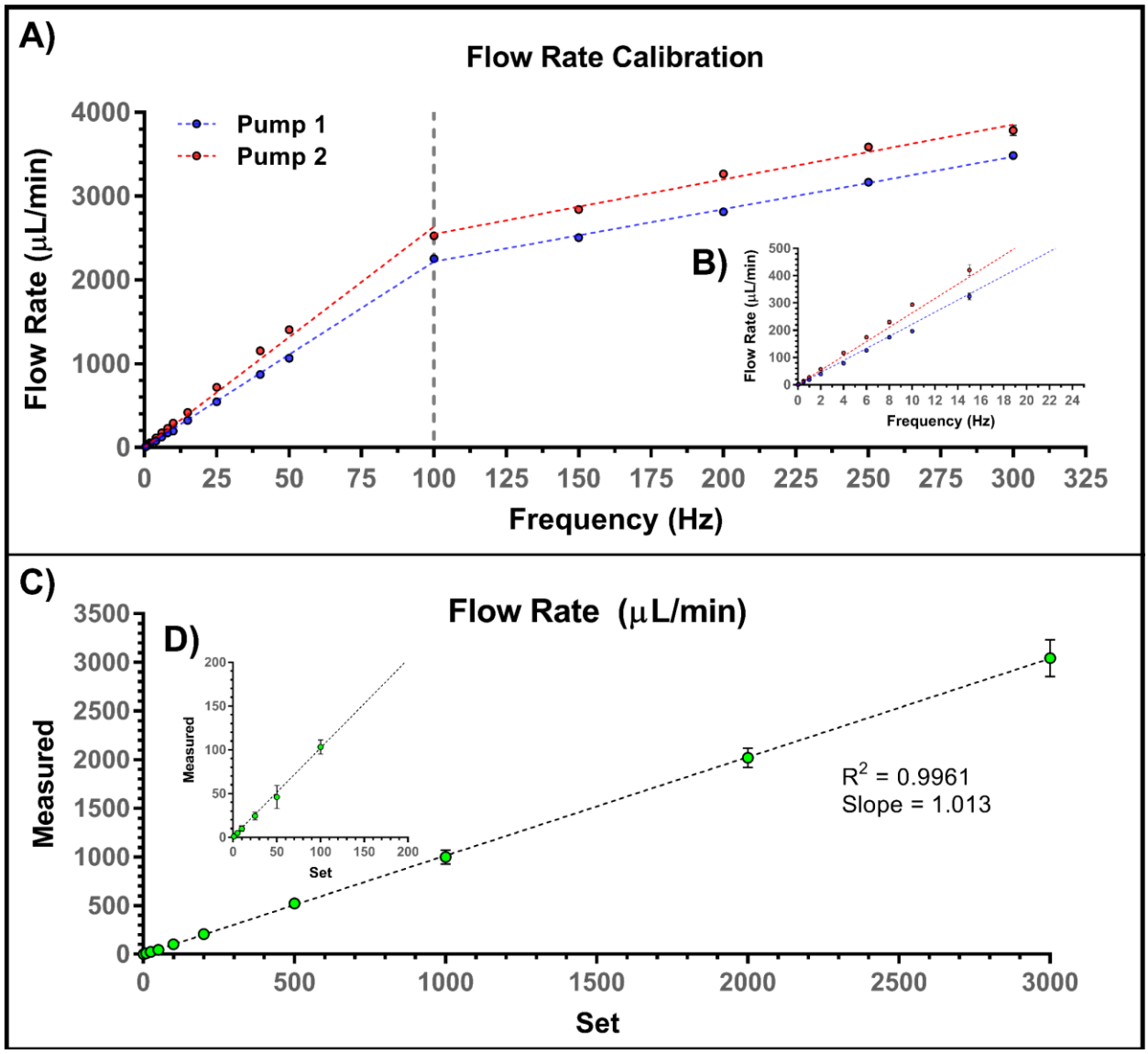

Figure 2: Calibration and Validation of Flow Rates. A) *Calibration curve for a MICCS module for each of the two pumps created by measuring the mass of water displaced at given set frequencies (n=3, error bars indicate standard deviation). The response exhibits two linear intervals from 0-100 Hz and from 100-300 Hz. Curve details not provided here as they need to be established*

for each set-up independently (see code for details). ***B)*** *Close-up of the low flow-rate region* ***C)*** *Validating the flow rates of the specific setup used for the subsequent experiments showed reproducible flow rates even down to 1 µL/min* ***(D)*** *(n=4, error bars indicate standard deviation).*

A 3D Printed Mixer and Computational Model Allow Precise Repeatable Dynamic Concentration Profiles

The ability to create dynamic flow waveforms has been crucial in many *in vitro* physiological studies such as those investigating effects of blood[32–34] and lymphatic shear stress[35,36]. Several systems have recently built on the ability to control flow dynamically or through valving techniques to create temporal concentration profiles[17,37–44]. While each of them is powerful for certain applications, we believe that the flexibility MICCS provides allows researchers to more easily accomplish this. MICCS can reliably produce any dynamic flow profile (<3,000 µL/min peak flow rate) by loading a custom ".csv" file containing the desired flow rates and time intervals. We chose here to demonstrate the improved functionality of MICCS by incorporating a microfluidic static mixer to create dynamic concentration profiles useful in many cell stimuli studies[13] whether the stimulus be drugs, glucose[45,46], hormones or growth factors[38,40]. By connecting one pump to a reservoir containing a concentrated solution and the other pump to a reservoir containing buffer solution, dynamically changing the ratio of the flow rate of one pump to the other, and mixing the flow from both pumps, we can dynamically control the concentration of a solute while keeping the flow rate constant (Fig. 3A). If needed, one can also have a dynamically changing flow rate. While there are many commercially available static mixers that can reliably mix two solutions, we chose to design our own, utilizing a 3D printed microfluidic mold[47–49], in order to demonstrate not only the functionality of MICCS, but also to show the ability of rapidly producing microfluidic devices for use with the system without the need for expensive microfabrication techniques such as photolithography[50] or micromachining[51]. The resulting device was composed of a series of interconnected triangles spanning the two inlets to the single outlet (Fig. 3B). The expansion of fluid intro the triangle region caused the formation of small vortices that assisted with mixing (Fig. S7). Before any experimental validation, we simulated the mixing of fluorescein with water at a 400 µL/min steady flow rate for each inlet (Fig. 3C) and showed that we achieve complete mixing after passing a minimal distance (Fig. 3D). Utilizing the same computational fluid dynamics (CFD) and solute transport model used for the constant flow above, we performed a parametric sweep over set values of inlet velocities to create dynamic concentration profiles. We found that our simulation accurately predicted the concentration profiles given our programmed flow rate values derived from the required concentration profiles (Fig. 3E). We chose to produce three different waveforms (ramp, sinusoid and pharmacokinetic-like) over a 10 minute period for validation. The user, however, can create profiles on any time scale (from seconds to weeks) depending on the volume,

stability, and other limiting factors of the solutions to be used. It is important to note that the used pumps were inherently pulsatile in nature with a stroke volume according to the manufacturer of around 2 µL. This pulsatility was not incorporated into the simulation as the phase difference between the two pumps cannot be controlled accurately, thus although the real concentration values at the output will likely be very similar to the simulation, the extent of spatial mixing along the length of the device might not necessarily be reflected accurately by the simulation in Fig. 3C. The computational model (see supplemental files), along with a microfluidic mixer, allows us to quickly validate the resulting output concentration profile for any given solute, temperature, inlet flow rates and duration thus reducing the need to validate these concentration profiles before an experiment through physical measurements of the solute which can be prohibitively costly, tedious and time-consuming.

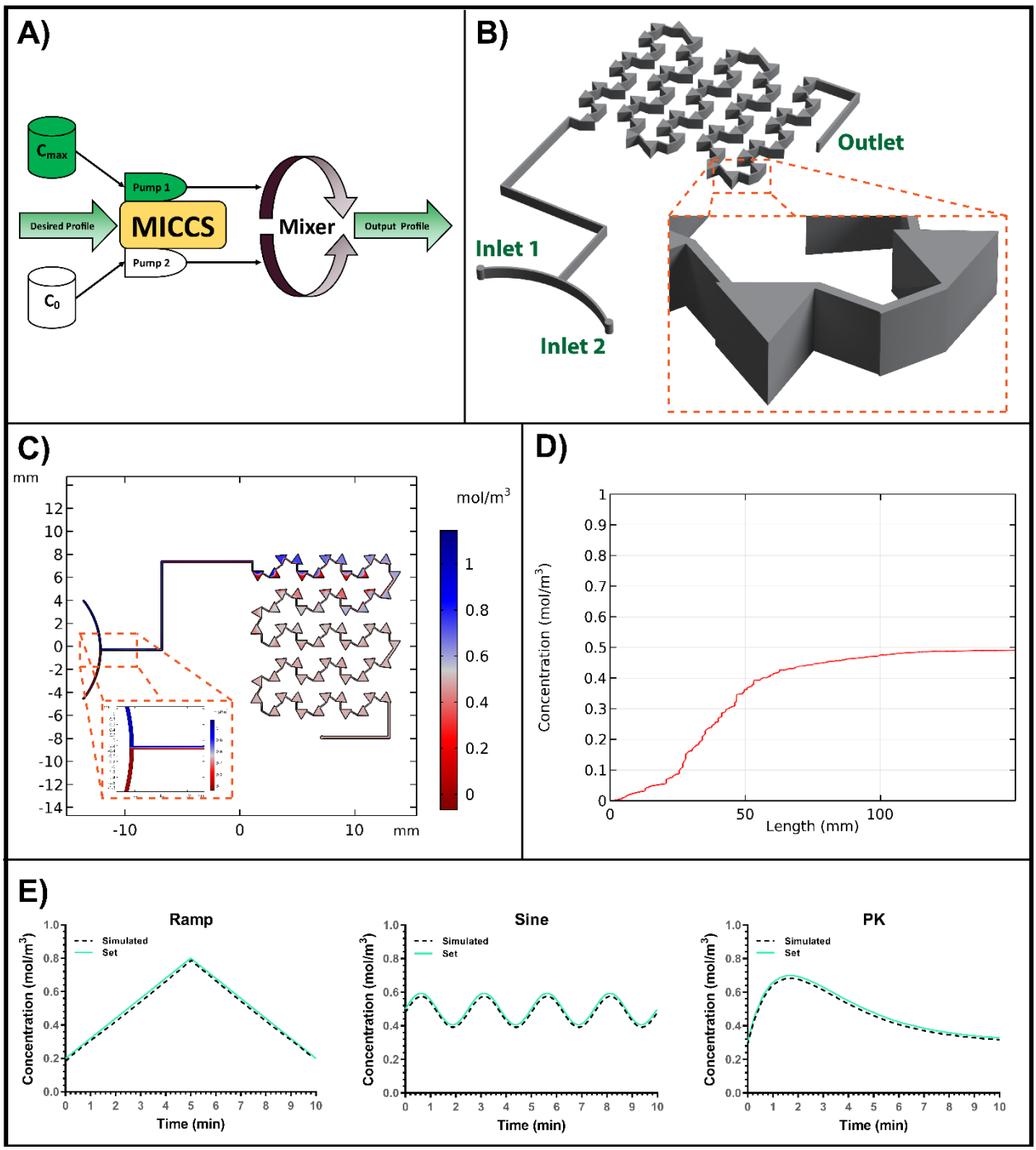

Figure 3: Dynamic Concentration Profiles using MICCS. A) *By utilizing two reservoirs, each connected to one of the pumps and then to a static efficient mixer, we can create dynamic concentration waveforms while holding the output flow rate constant.* ***B)*** *A CAD model of our microfluidic mixer that can handle a large range of input flow rates from a few µL/min to 3,000 µL/min and above.* ***C)*** *A CFD simulation showing efficient mixing of fluorescein at 37 °C under 400 µL/min flow rates for each of the inlets.* ***D)*** *Full mixing occurs after 125 mm at these given flow rates.* ***E)*** *The developed CFD model allows us to computationally validate that our prescribed flow waveforms create the desired concentration profiles, thus minimizing the need for real measurement-based validation before a stimulation experiment.*

In addition to dynamically perturbing mono-cultures of cells to probe for mechanistic insights, being able to easily prescribe dynamic concentration profiles offers new capabilities for stimulating organ-on-chip

and microphysiological systems,. By uploading a ".csv" file, we can recreate any arbitrarily defined concentration profile. Our typical setup used two 250 mL bottles as reservoirs which connected to a MICCS module using silicone tubing (Fig. 4A). With the same flow rate values used in the simulations, we achieved the same concentration profiles predicted by the computational model when measuring fluorescence intensity of fluorescein. The concentration profiles were highly accurate and reproducible (Fig. 4B). Additionally, the modularity and programmability of the system allows researchers to expose their cultures to any number of different solute concentrations and flow-rate profiles with minimal user intervention.

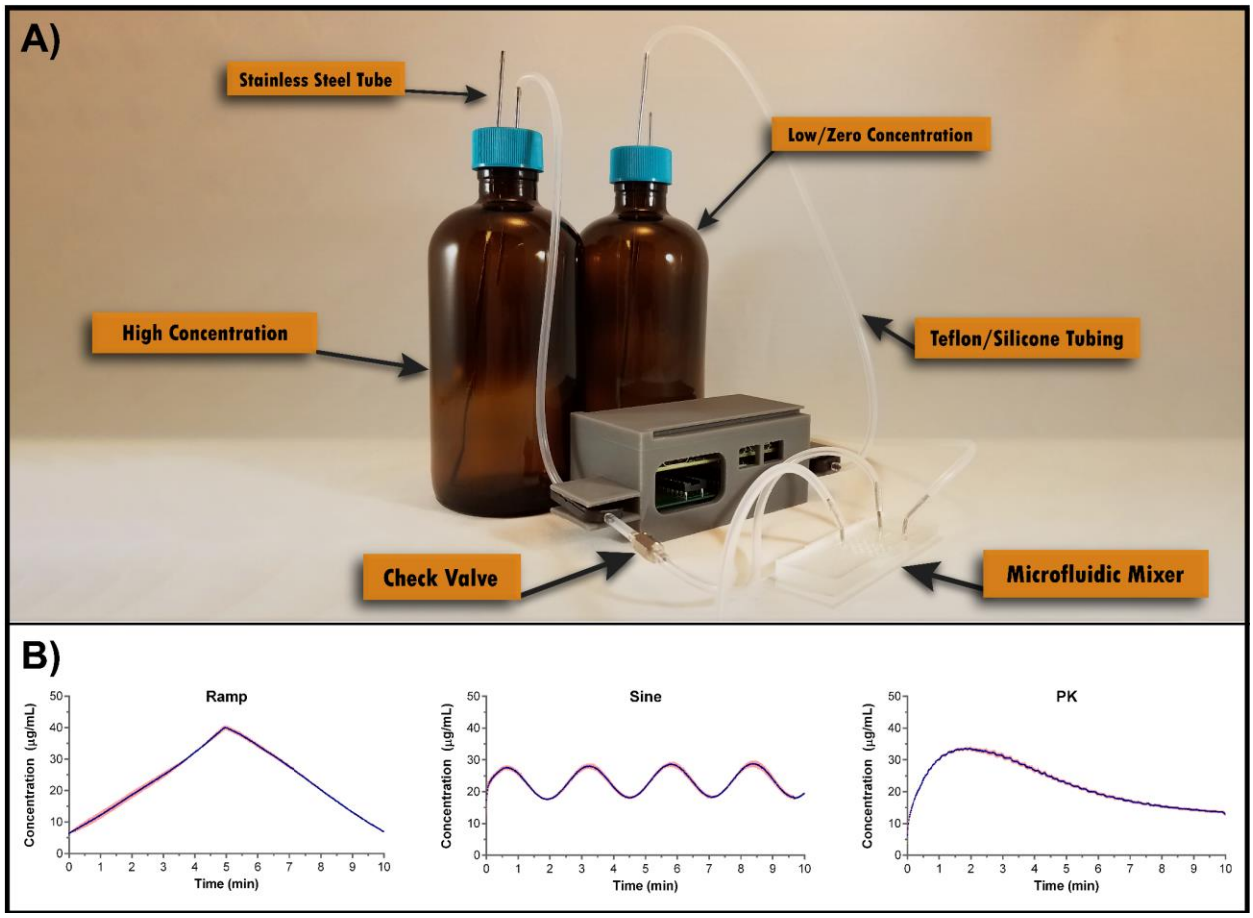

Figure 4: Generating dynamic concentration profiles using MICCS. A) *Our typical setup for generating a concentration profile for a single solute. Each pump is connected to a separate reservoir containing the lower and upper limits of the required concentration profile. The flow-rate ratio is then modulated to create the concentration profile at the output of the microfluidic mixer. A unidirectional valve is added to prohibit backflow and make the setup more robust against back pressures. Both silicone and Teflon tubing can be used for the connections. Additionally, thermoplastic-based commercially available mixers can be used in place of our PDMS mixer.* ***B)*** *Examples of the experimental concentration profiles generated using fluorescein. The mean is represented in blue while the red bands represent the standard deviation. N=3.*

Potential Applications

MICCS opens up the possibility to automate a variety of biological protocols. Such procedures include but are not limited to:

1- Conducting stimulation or washing assays such as the commonly used glucose stimulated insulin secretion (GSIS) assay for assessing pancreatic islet function in a reproducible and controlled manner.
2- Automating media exchange by running the *constant_flow* function for a specific duration with a given time delay (for discrete media changes) or by continuously running at a fixed flow rate for continuous perfusion.
3- Using multiple MICCS modules to create complex stimulation experiments with a custom ".csv" file. Experiments requiring the ability to mimic hormonal profiles of various hormones at the same time, blood serum concentration levels of a particular molecule over time, pharmacokinetic (PK) profiles and meal-related exposures are all possible with MICCS.
4- Remotely stimulating a culture or media condition from any internet enabled device using a VNC client.
5- Mimicking physiologically relevant blood flow through an endothelialized channel with a programed pulsatile heart-like flow rate.
6- Mimicking physiologically relevant lymphatic flow by using *in vivo* measured flow rates[52,53].

Current Limitations

MICCS offers a variety of features and capabilities that are highly desirable to researchers utilizing any kind of fluidic control. There are a few limitations, however, that could be addressed with different designs in the future; 1) Depending on the geometry of the microfluidic device MICCS is connected to, the flow rates might prove to be too high for certain applications especially those involving very small channels and shear-sensitive cells. While MICCS can achieve flow rates as low as 1 µL/min, the minimum reliable flow rate highly depends on the setup, including the overall resistance, back pressure and fluid being pumped. Through extended use, we found that the lowest reliable flow rate that can be used with our setup was around 50 µL/min. 2) The current setup uses silicone tubing and a PDMS-based mixer, and while these can be used for a variety of applications, they should not be used in experiments that involve hormones or drugs as silicone and PDMS tend to be highly absorbent[54–56]. An easy solution is to use Teflon tubing and a commercially available mixer made from polystyrene or other minimally absorbent plastics.

Conclusions

We presented a low-cost (<$200 USD), modular, scalable, fully-programmable and easy to assemble pumping platform that can be used for a variety of fluidic applications, providing all the necessary design and control files to fully implement under an open-source license. We believe our open-source MICCS system will be valuable to both biological and non-biological researchers, and we look forward to seeing how it will be improved in collaboration with the scientific community.

Acknowledgements

The authors would like to thank the wider microfluidics community and various researchers that provided both direct and indirect input for the design specifications of MICCS. This work was funded under the Defense Advanced Projects Agency (DARPA) Microphysiological Systems Program (W911NF-12-2-0039).

References

1 A. Skardal, T. Shupe and A. Atala, *Drug Discov. Today*, 2016, **21**, 1399–1411.

2 D. A. Tagle, C. Livingston and K. M. Fabre, *Exp. Biol. Med.*, 2014, **239**, 1073–1077.

3 E. W. Esch, A. Bahinski and D. Huh, *Nat. Rev. Drug Discov.*, 2015, **14**, 248–260.

4 P. N. Joshi, in *Lab-on-a-Chip Fabrication and Application*, InTech, 2016, pp. 77–123.

5 U. Marx, T. B. Andersson, A. Bahinski, M. Beilmann, S. Beken, F. R. Cassee, M. Cirit, M. Daneshian, S. Fitzpatrick, O. Frey, C. Gaertner, C. Giese, L. Griffith, T. Hartung, M. B. Heringa, J. Hoeng, W. H. De Jong, H. Kojima, J. Kuehnl, M. Leist, A. Luch, I. Maschmeyer, D. Sakharov, A. J. A. M. Sips, T. Steger-Hartmann, D. A. Tagle, A. Tonevitsky, T. Tralau, S. Tsyb, A. Van De Stolpe, R. Vandebriel, P. Vulto, J. Wang, J. Wiest, M. Rodenburg and A. Roth, *ALTEX*, 2016, **33**, 272–321.

6 S. N. Bhatia and D. E. Ingber, *Nat. Biotechnol.*, 2014, **32**, 760–772.

7 F. Zheng, F. Fu, Y. Cheng, C. Wang, Y. Zhao and Z. Gu, *Small*, 2016, **12**, 2253–2282.

8 L. G. Griffith and M. A. Swartz, *Nat. Rev. Mol. Cell Biol.*, 2006, **7**, 211–224.

9 M. Baker, *Nature*, 2011, **471**, 661–665.

10 V. van Duinen, S. J. Trietsch, J. Joore, P. Vulto and T. Hankemeier, *Curr. Opin. Biotechnol.*, 2015, **35**, 118–126.

11 J. P. Wikswo, *Exp. Biol. Med.*, 2014, **239**, 1061–1072.

12 J. P. Wikswo, F. E. Block, D. E. Cliffel, C. R. Goodwin, C. C. Marasco, D. A. Markov, D. L. McLean, J. A. McLean, J. R. McKenzie, R. S. Reiserer, P. C. Samson, D. K. Schaffer, K. T. Seale and S. D. Sherrod, *IEEE Trans. Biomed. Eng.*, 2013, **60**, 682–690.

13 A. Jovic, B. Howell and S. Takayama, *Microfluid. Nanofluidics*, 2009, **6**, 717–729.

14 H. J. Kim, D. Huh, G. Hamilton and D. E. Ingber, *Lab Chip*, 2012, **12**, 2165.

15 D. Huh, B. D. Matthews, A. Mammoto, M. Montoya-Zavala, H. Y. Hsin and D. E. Ingber, *Science (80-.).*, 2010, **328**, 1662–1668.

16 C. K. Byun, K. Abi-Samra, Y.-K. Cho and S. Takayama, *Electrophoresis*, 2014, **35**, 245–257.

17 G. A. Cooksey, C. G. Sip and A. Folch, *Lab Chip*, 2009, **9**, 417–426.

18 F. Abhari, H. Jaafar and N. A. Md Yunus, *Int. J. Electrochem. Sci.*, 2012, **7**, 9765–9780.

19 B. Wijnen, E. J. Hunt, G. C. Anzalone and J. M. Pearce, *PLoS One*, 2014, **9**, 1–8.

20 J. R. Lake, K. C. Heyde and W. C. Ruder, *PLoS One*, 2017, **12**, 1–12.

21 P. Frank, S. Haefner, M. Elstner and A. Richter, *Inventions*, 2016, **1**, 13.

22 T. Satoh, G. Narazaki, R. Sugita, H. Kobayashi, S. Sugiura and T. Kanamori, *Lab Chip*, 2016, **16**, 2339–2348.

23 L. J. Y. Ong, L. H. Chong, L. Jin, P. K. Singh, P. S. Lee, H. Yu, A. Ananthanarayanan, H. L. Leo and Y.-C. Toh, *Biotechnol. Bioeng.*, 2017, **114**, 2360–2370.

24 C. Morris, D. J. Banks, L. Gaweda, S. Scott, X. X. Zhu, M. Panico, P. Georgiou and C. Toumazou, in *Proceedings of the Annual International Conference of the IEEE Engineering in Medicine and Biology Society, EMBS*, IEEE, 2011, pp. 8412–8415.

25 A. Rountree, A. Karkamkar, G. Khalil, A. Folch, D. L. Cook and I. R. Sweet, *Heliyon*, 2016, **2**, e00210.

26 P. G. Miller and M. L. Shuler, *Biotechnol. Bioeng.*, 2016, **113**, 2213–2227.

27 W. Inman, K. Domansky, J. Serdy, B. Owens, D. Trumper and L. G. Griffith, *J. Micromechanics Microengineering*, 2007, **17**, 891–899.

28 T. Bharambe, P. W. Mogal and S. Patil, 2016, 490–495.

29 C. T. Culbertson, S. C. Jacobson and J. Michael Ramsey, *Talanta*, 2002, **56**, 365–373.

30 M. Woelfle, P. Olliaro and M. H. Todd, *Nat. Chem.*, 2011, **3**, 745–748.

31 T. Sherratt and G. Roberts, *Science (80-.).*, 2012, **337**, 1304–1305.

32 N. Resnick, H. Yahav, A. Shay-Salit, M. Shushy, S. Schubert, L. C. M. Zilberman and E. Wofovitz, *Prog. Biophys. Mol. Biol.*, 2003, **81**, 177–199.

33 D. Lu and G. S. Kassab, *J. R. Soc. Interface*, 2011, **8**, 1379–85.

34 H. E. Abaci, Y.-I. Shen, S. Tan and S. Gerecht, *Sci. Rep.*, 2015, **4**, 4951.

35 A. Sabine, C. Saygili Demir and T. V. Petrova, *Antioxid. Redox Signal.*, 2016, **25**, 451–465.

36 J. A. Kornuta and J. B. Dixon, *Ann. Biomed. Eng.*, 2014, **42**, 1691–1704.

37 D. W. Lee, I. Doh, Y. Kim and Y.-H. Cho, *Lab Chip*, 2013, **13**, 3658.

38 N. B. Whitticar, E. W. Strahler, P. Rajan, S. Kaya and C. S. Nunemaker, *Biol. Proced. Online*, 2016, **18**, 19.

39 Y. Kim, S. D. Joshi, W. C. Messner, P. R. LeDuc and L. A. Davidson, *PLoS One*, 2011, **6**, e14624.

40 F. Lin, W. Saadi, S. W. Rhee, S.-J. Wang, S. Mittal and N. L. Jeon, *Lab Chip*, 2004, **4**, 164.

41 D. W. Lee and Y.-H. Cho, *Lab Chip*, 2009, **9**, 1681.

42 X. Zhang and M. G. Roper, *Anal. Chem.*, 2009, **81**, 1162–1168.

43 A. F. Adewola, D. Lee, T. Harvat, J. Mohammed, D. T. Eddington, J. Oberholzer and Y. Wang, *Biomed. Microdevices*, 2010, **12**, 409–417.

44 M. Sumit, S. Takayama and J. J. Linderman, *Integr. Biol.*, 2017, **9**, 6–21.

45 X. Li, J. C. Brooks, J. Hu, K. I. Ford and C. J. Easley, *Lab Chip*, 2017, **208**, 501–512.

46 Y. H. Hsiao, C. H. Hsu and C. Chen, *Molecules*, 2016, **21**, 896.

47 G. Comina, A. Suska and D. Filippini, *Lab Chip*, 2014, **14**, 424–430.

48 Y. Hwang, O. H. Paydar and R. N. Candler, *Sensors Actuators, A Phys.*, 2015, **226**, 137–142.

49 K. ichiro Kamei, Y. Mashimo, Y. Koyama, C. Fockenberg, M. Nakashima, M. Nakajima, J. Li and Y. Chen, *Biomed. Microdevices*, 2015, **17**, 36.

50 G. M. Whitesides, E. Ostuni, S. Takayama, X. Jiang and D. E. Ingber, *Annu. Rev. Biomed. Eng.*, 2001, **3**, 335–373.

51 D. J. Guckenberger, T. E. de Groot, A. M. D. Wan, D. J. Beebe and E. W. K. Young, *Lab Chip*, 2015, **15**, 2364–2378.

52 T. Kassis, S. C. Yarlagadda, A. B. Kohan, P. Tso, V. Breedveld and J. B. Dixon, *Am. J. Physiol. Gastrointest. Liver Physiol.*, 2016, **310**, ajpgi.00318.2015.

53 T. Kassis, A. B. Kohan, M. J. Weiler, M. E. Nipper, R. Cornelius, P. Tso and J. B. Dixon, *J. Biomed. Opt.*, 2012, **17**, 86005.

54 S. Halldorsson, E. Lucumi, R. Gómez-Sjöberg and R. M. T. Fleming, *Biosens. Bioelectron.*, 2015, **63**, 218–231.

55 K. J. Regehr, M. Domenech, J. T. Koepsel, K. C. Carver, S. J. Ellison-Zelski, W. L. Murphy, L. A. Schuler, E. T. Alarid and D. J. Beebe, *Lab Chip*, 2009, **9**, 2132.

56 P. M. Van Midwoud, A. Janse, M. T. Merema, G. M. M. Groothuis and E. Verpoorte, *Anal. Chem.*, 2012, **84**, 3938–3944.